



Common Spatial Pattern EEG decomposition for Phantom Limb Pain detection

Downloaded from: <https://research.chalmers.se>, 2026-04-14 13:04 UTC

Citation for the original published paper (version of record):

Lendaro, E., Balouji, E., Baca, K. et al (2021). Common Spatial Pattern EEG decomposition for Phantom Limb Pain detection. Proceedings of the Annual International Conference of the IEEE Engineering in Medicine and Biology Society, EMBS, 2021-January: 726-729.
<http://dx.doi.org/10.1109/EMBC46164.2021.9630561>

N.B. When citing this work, cite the original published paper.

© 2021 IEEE. Personal use of this material is permitted. Permission from IEEE must be obtained for all other uses, in any current or future media, including reprinting/republishing this material for advertising or promotional purposes, or reuse of any copyrighted component of this work in other works.

(article starts on next page)

Common Spatial Pattern EEG decomposition for Phantom Limb Pain detection.

Eva Lendaro, Ebrahim Balouji, Karen Baca, Azam Sheikh Muhammad and Max Ortiz-Catalan

Abstract—Phantom Limb Pain (PLP) is a chronic condition frequent among individuals with acquired amputation. PLP has been often investigated with the use of functional MRI focusing on the changes that take place in the sensorimotor cortex after amputation. In the present study, we investigated whether a different type of data, namely electroencephalographic (EEG) recordings, can be used to study the condition. We acquired resting state EEG data from people with and without PLP and then used machine learning for a binary classification task that differentiates the two. Common Spatial Pattern (CSP) decomposition was used as the feature extraction method and two validation schemes were followed for the classification task. Six classifiers (LDA, Log, QDA, LinearSVC, SVC and RF) were optimized through grid search and their performance compared. Two validation approaches, namely all-subjects validation and leave-one-out cross-validation (LOOCV), resulted in high classification accuracy. Most notably, the 93.7% accuracy achieved with SVC in LOOCV holds promise for good diagnostic capabilities using EEG biomarkers. In conclusion, our findings indicate that EEG data is a promising target for future research aiming at elucidating the neural mechanisms underlying PLP and its diagnosis.

I. INTRODUCTION

People suffering peripheral nerve damage often report neuropathic pain, which is particularly difficult to treat. Amputation, as the most extreme case of nerve injury, is frequently associated with the presence of phantom limb pain (PLP): the perception of pain in the missing limb [1][2]. A large body of literature on PLP has identified a relationship between PLP and maladaptive changes taking place specifically in the primary somatosensory and motor cortex [3]. However, chronic pain is a complex integrative phenomenon that results from interaction between sensory, cognitive, emotional, and motivational processes [4] and presents complex comorbidities such as anxiety and depression[5]. PLP is associated with the activation of an extended brain network that goes beyond the sensorimotor

This work was supported by the Promobilia Foundation, the IngaBritt and Arne Lundbergs Foundation, the Swedish Innovation Agency (VINNOVA), and the Swedish Research Council (Vetenskapsrådet).

E. Lendaro is with the Center for Bionics and Pain Research, Sweden, and with the Department of Electrical Engineering, Chalmers University of Technology, Sweden lendaro@chalmers.se

E. Balouji is with the Department of Electrical Engineering, Chalmers University of Technology, Sweden balouji@chalmers.se

K. Baca and A.S. Muhammad are with the Department of Computer Science and Engineering, Chalmers University of Technology, Sweden karenb@chalmers.se, azams@chalmers.se

M. Ortiz-Catalan is with the Center for Bionics and Pain Research, Sweden, with the Department of Electrical Engineering, Chalmers University of Technology, Sweden, with the Operational Area 3, Sahlgrenska University Hospital, Sweden, and with the Department of Orthopaedics, Institute of Clinical Sciences, Sahlgrenska Academy, University of Gothenburg, Sweden maxo@chalmers.se

circuitry [6], and this must be taken into account when investigating its neural basis. Although anatomical connections are one route for integration, dynamically mutable functional connections are likely implicated in the dynamic pain connectome [7], mediating pain perception and neural oscillations ("brain rhythms") have been shown to be a medium subserving such integration [8]. Studies on the neural basis of PLP have mostly used functional magnetic resonance imaging (fMRI) [9], which has a coarse temporal resolution (2-3 s) and is unsuitable to study oscillations at frequencies higher than 0.5 Hz. At present, no study has investigated electroencephalographic (EEG) rhythms in subjects suffering from PLP. More generally, pain-related changes have been observed in brain rhythms at frequencies across the entire EEG spectrum (from infra-slow, at 0.1Hz, to gamma oscillations, at 100Hz) [10]. When it comes to chronic pain specifically, a rather conventional approach has been to analyse quantitatively the power spectral density of resting state EEG over relatively long epochs [11]. This approach has been criticised for both overlooking power fluctuation in shorter time scales and for not showing statistically significant differences between pathological and healthy EEG after correction for multiple comparisons [12]. In recent years however, EEG data has been increasingly used in combination with machine learning (ML) techniques for diagnostic purposes (e.g. epilepsy, strokes, Alzheimer's disease, etc) [13]. Apart from the obvious value within diagnostics, techniques allowing for automatic abnormal EEG detection could lead to the derivation of EEG-based chronic pain markers. ML methods can be categorized into feature-based (with handcrafted, a priori selected features), and end-to-end approaches (with learned features). Feature-based ML has been widely used for non-invasive Brain Computer Interfaces (BCIs), where a popular method to extract features is through the use of the common spatial patterns (CSP) algorithm. CSP in the context of EEG was described by Koles et al. [14], who initially conceived it as a way to extract abnormal components in clinical EEG and to visualize their topography. Only recently has the algorithm been used to extract features for neurological disease diagnostics [15]. In substance, CSP is a supervised source separation method based on the assumption that the sources are uncorrelated Gaussian distributions belonging to two distinct classes. In particular, CSP is a dimensionality reduction technique that aims at designing spatial filters that maximize the variance of the spatially filtered signal under one condition while minimizing it for the other condition. A comprehensive tutorial on CSP can be found in [16]. The

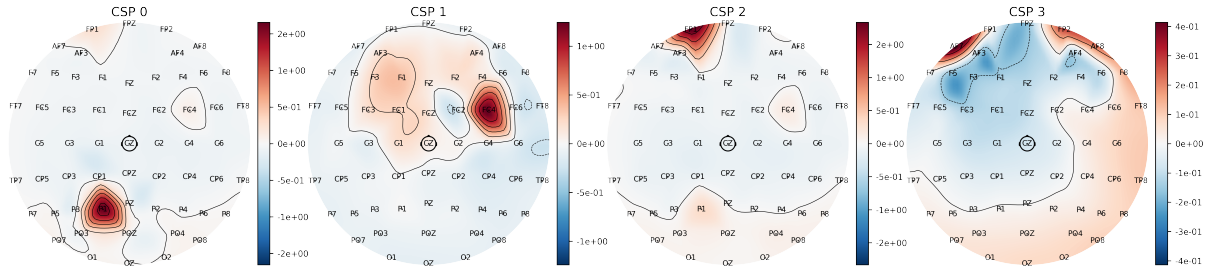


Fig. 1. Example of spatial patterns (forward model of the sources) derived from CSP decomposition into four components using the training data from one of the *all-subjects* validation schema. The patterns are displayed in an alternated fashion, from left to right showing the topographical distribution of the largest variance for the *Pain* class in CSP0, followed by the largest variance for the *No Pain* class in CSP1, second to largest for *Pain* in CSP2 and lastly second to largest for *No Pain* in CSP3. On the scalp topography are the channels labels also visible: the largest variance peaks at P2 for CSP0, FC4 for CSP1, FP1 for CSP2 and AF7 for CSP3.

TABLE I
PARTICIPANTS INFORMATION

Subject ID	Sex	Age	Amputation type	# Epochs
NP1	F	41	TR	326
P2	M	57	TT	301
P3	M	50	TH	155
P4	M	49	TH	272
P5	M	65	TH	173
P6	F	44	TR	147
P9	M	18	TH	273
P10	M	34	TF	181
P11	F	60	TR-b/TT-b	290
NP12	M	44	TR-b/TT-b	514
P14	M	44	TT	169
NP16	M	45	TH	530
P18	F	43	TT	199
P19	M	74	TT	339
P20	M	63	TF-b	181
NP21	M	43	TR	362
NP24	M	46	TH	362
NP25	F	39	TF	362
P26	F	38	TF	362
P27	M	54	TF	362
NP32	M	24	TR	211
NP33	M	76	TT	362
NP51	M	45	TH	362
P52	M	54	TF	181
P54	M	54	TH	362
NP57	M	58	TT	362

primary question we seek to answer with the present study is whether EEG data contain relevant information for the study and diagnosis of PLP. We answer this question by setting up the problem as a classification task. Specifically, we record EEG from subjects with acquired amputation, with and without PLP and explore the use of different machine learning classifiers for the discrimination of these two classes using CSP based features. Further, we display topographic maps extracted using CSP filtering, which is of particular interest for the broader scope of our application. Our ultimate goal is not limited to mere classification of abnormal signals, but it extends to the exploration of whether EEG patterns can be used as markers for PLP.

II. METHODOLOGY

A. PLP dataset

The study was approved by the Swedish Ethical Review Authority (Dnr 041-17, T652-17) and all participants provided written informed consent. A total of 26 adults subjects with acquired limb deficiency were enrolled on a voluntary basis and assigned to one of two groups (*Pain*

or *No Pain*, based on whether they suffered from PLP). Details on the participants are reported in Table I: subject IDs starting with the letter *P* indicate those belonging to the *Pain* group while *NP* demarcates the ID of those in the *No Pain* group. Age at recording (years) and amputation type (*TR* - transradial, *TH* - transhumeral, *TT* - transtibial, *TF* - transfemoral, and the suffix *-b* indicating bilateral amputations) are also denoted. EEG was recorded using a 58-channel referential montage (visible in Figure 1), with active electrodes fixed in a cap at the standard 10-20 positions and AFz as ground (g.HIamp, g.tec medical engineering GmbH, Austria). During the recording, subjects rested with their eyes closed sitting comfortably on a chair in a quiet room for sessions of variable length between 5 and 7 minutes. Some participants underwent multiple recording sessions on different days. Signals were sampled at 2400Hz.

B. Preprocessing

The preprocessing was carried out using custom MATLAB scripts and EEGLAB functions [17]. The steps, in order, were: resampling a 256Hz, 50Hz powerline removal with CleanLine (EEGLAB plugin), and re-referencing to common average. The data were then bandpass filtered between 4 and 40Hz and segmented in 2-second non-overlapping EEG epochs. 4 Hz was chosen as lower cutoff frequency in order to minimize possible artifact. The first and last 30 seconds of every recording session were discarded. Table I contains information regarding the number of epochs used for each subject. The remainder of the analyses was carried out in Python.

TABLE II
ALL-SUBJECTS VALIDATION PERFORMANCE (%)

	LDA	LinearSVC	Log	QDA	RF	SVC
Accuracy	83.82 (0.79)	87.89 (0.81)	87.91 (0.82)	88.76 (0.91)	99.76 (0.15)	98.16 (0.41)
Precision	81.89 (2.77)	87.23 (1.23)	87.15 (1.13)	82.29 (1.29)	99.59 (0.29)	97.49 (0.54)
Recall	88.15 (4.68)	89.45 (1.04)	89.6 (0.91)	99.48 (0.19)	99.95 (0.07)	98.95 (0.39)
F1-score	84.76 (0.99)	88.32 (0.75)	88.36 (0.76)	90.07 (0.72)	99.77 (0.15)	98.22 (0.40)
Entropy	10.63 (0.78)	11.69 (1.00)	12.02 (0.89)	6.88 (1.11)	0.5 (0.27)	2.96 (0.64)

TABLE III
LEAVE ONE OUT CROSS VALIDATION PERFORMANCE (%)

	LDA	LinearSVC	Log	QDA	RF	SVC
Accuracy	74.4	74.9	75.2	82.4	92.4	93.7
Precision	72.0	74.2	74.5	76.3	92.5	92.7
Recall	82.1	78.2	78.5	95.1	92.7	95.3
F1-score	76.7	76.1	76.4	84.7	92.6	94.0
Entropy	7.9	11.1	11.4	8.3	9.8	7.1

C. Feature extraction

Functions from the MNE-python package [18] were used to carry out the CSP based feature extraction. Briefly, CSP is a technique that takes multichannel data in the original filter space belonging to two classes (here Pain and No Pain) and decomposes them into additive components in a surrogate source space. The optimization criterion used to determine the CSP is to maximize the variance of the spatially filtered signal under one condition while minimizing it for the other condition. In this study, we have decomposed the signals into 4 components. Training data were used to estimate the filters that were then applied to the test set. For every epoch, the average power of the data in the CSP space was taken as representative feature.

TABLE IV
BEST HYPERPARAMETERS

	Best Hyperparameters	Count
LDA	'shrinkage': None, 'solver': 'eigen'	17
LinearSVC	'C': 0.1, 'penalty': 'l1'	11
Log	'C': 0.2, 'penalty': 'l1', 'solver': 'saga'	6
QDA	reg_param': 0.05	25
RF	'max_depth': None, 'max_features': 2, 'min_samples_split': 5, 'n_estimators': 100	9
SVC	C': 5, 'gamma': 0.5, 'kernel': 'rbf'	6

D. Validation schemes and classification

The cross validation and classification part of the study were implemented with the use of two different validation schemes. In the first approach a repeated random subsampling validation was carried out: the epochs from each recording session were randomly divided into training and test sets, with 80% of the epochs allocated to the training set and 20% of the epochs allocated to the test set. In this way, data from all the subjects and all the recording sessions were used to estimate the filters for CSP extraction (*all-subjects* validation). The validation was iterated 10 times. The second approach consisted in a Leave One Out Cross Validation (*LOOCV*) scheme, where one subject at a time was left out from the training set and excluded from the estimation of the spatial filters. Six different classifiers were used and compared. The classifiers adopted respectively were Linear Discriminant Analysis (LDA), Logistic Regression (Log), Quadratic Discriminant Analysis (QDA), Linear Support Vector Classification (LinearSVC), C-Support Vector Classification (SVC) and Random Forest Classifier (RF)

(built using Scikit-Learn [19]). Fine tuning of the hyperparameters was carried out through grid search, in which for given values of the parameters, all combinations were considered. By exhaustively searching the hyper-parameter space we are certain of reaching the best cross validation scores for a given training/test partition. In the *LOOCV* approach, a random 20% of the epochs in each recording sessions was withheld from all the participants (including the test subject) in order to carry out the grid search.

III. RESULTS

The number of epochs for every subject is reported in Table I. The dataset is well balanced presenting 3753 epochs in the *No Pain* class and 3947 epochs in the *Pain* class. Figure 1 illustrate the patterns derived from the CSP decomposition in the *all-subjects* validation into four components, where filters have been estimated using a random 80% of the epochs from all the recording sessions and using all participants. Table II and Table III report the performance metrics for the six classifiers tested for the *all-subjects* validation and *LOOCV* respectively. In addition to the classical performance metrics (Accuracy, Precision, Recall and F1-score) also Entropy is given as a measure of the stability of the classification over time, where high entropy indicates a model making unstable predictions. Finally, Table IV specifies the results of the hyperparameter grid search (conducted with a Scikit-Learn function [19]) on the *LOOCV* scheme. The grid search exhaustively generates candidates from a grid of specified parameter values, considering all their combinations. The parameters are specified when building a classifier with Scikit-Learn. The results presented here are expressed in terms of count of how many times the same combination of parameters yielded the best performance over the 26 folds of the *LOOCV*: the combinations with the highest counts are reported for every classifier.

IV. DISCUSSION AND CONCLUSIONS

In this study we have investigated whether it is possible to use EEG recordings to discriminate between people with and without PLP. In order to achieve this, we decomposed the EEG into four CSP components and used their average power over 2-second epochs for the classification task. The results demonstrate the feasibility of this approach, even in a *LOOCV* setting, which is amenable to medical diagnostics. In clinical practice, the objectives could be for example to detect the presence of pain or to determine its magnitude in patients in which this information is not known. One of the reasons for choosing the CSP technique for feature extraction is its capacity of visualizing the patterns that yield the best classification accuracy (projections of the different components) as scalp topographic maps (see Figure 1). Note that this is a different approach from solving the inverse problem aimed at localizing the 3D signal sources, which could be carried out using the identified patterns. One limitation of our results at present is that before decomposition, the signals had been bandpassed filtered between 4 and 40Hz and it includes almost all the different frequency bands contained in

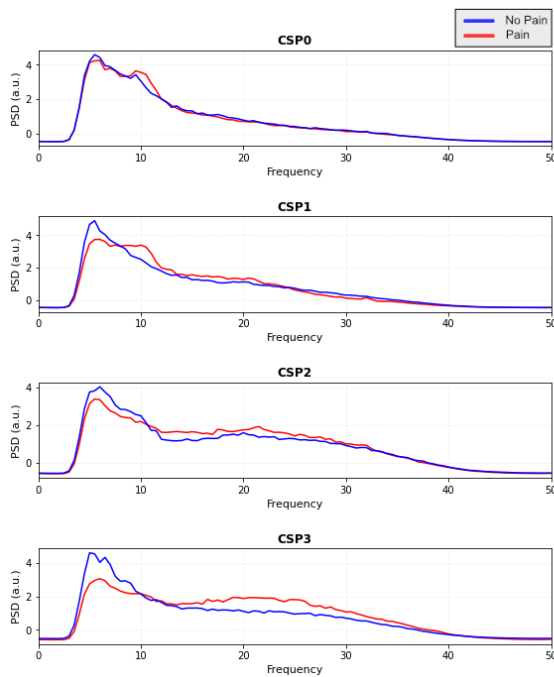


Fig. 2. Grand average of the power spectral density at four CSP components for the Pain group (in red) and the No Pain group (in blue).

EEG (theta (4–7 Hz), alpha (8–13 Hz), beta (14–29 Hz) and part of gamma (30–100 Hz)) (note, the delta band was left out). The reason for using such broad bandpass filtering was due to the exploratory nature of our analysis. By inspecting the grand average of the power spectral density of the four CSP components identified for the two classes (see Figure 2), it is possible to see how different spatial patterns might emerge considering separately narrower frequency bands (i.e. delta, theta, alpha, etc). Future studies could achieve this by employing the Filter Bank CSP [20], which is essentially CSP applied to the separate frequency bands extracted in the preprocessing step. A further step in the direction of exploring the neural correlates of PLP could then be to localize the sources yielding high classification accuracy by solving the inverse problem. Taken all these considerations together, EEG data seem a promising target for future research aiming at elucidating the neural mechanisms underlying PLP.

REFERENCES

- [1] M. Ortiz-Catalan, “The stochastic entanglement and phantom motor execution hypotheses: A theoretical framework for the origin and treatment of phantom limb pain,” *Frontiers in Neurology*, vol. 9, Sep. 2018. [Online]. Available: <https://doi.org/10.3389/fneur.2018.00748>
- [2] G. DI PINO, V. PIOMBINO, M. CARASSITI, and M. ORTIZ-CATALAN, “Neurophysiological models of phantom limb pain: what can be learnt,” *Minerva Anestesiologica*, vol. 87, no. 4, Apr. 2021. [Online]. Available: <https://doi.org/10.23736/S0375-9393.20.15067-3>
- [3] T. R. Makin and H. Flor, “Brain (re)organisation following amputation: Implications for phantom limb pain,” *NeuroImage*, vol. 218, p. 116943, 2020. [Online]. Available: <https://www.sciencedirect.com/science/article/pii/S1053811920304298>
- [4] R. Melzack, “Pain and the neuromatrix in the brain,” *Journal of dental education*, vol. 65, no. 12, p. 1378–1382, December 2001. [Online]. Available: <http://europepmc.org/abstract/MED/11780656>

- [5] X. Fuchs, H. Flor, and R. Bekrater-Bodmann, “Psychological factors associated with phantom limb pain: A review of recent findings,” *Pain Research and Management*, vol. 2018, pp. 1–12, Jun. 2018. [Online]. Available: <https://doi.org/10.1155/2018/5080123>
- [6] H. Flor and J. Andoh, “Origin of phantom limb pain: A dynamic network perspective,” *e-Neuroforum*, vol. 23, no. 3, Jan. 2017. [Online]. Available: <https://doi.org/10.1515/nf-2017-a018>
- [7] A. Kucyi and K. D. Davis, “The dynamic pain connectome,” *Trends in Neurosciences*, vol. 38, no. 2, pp. 86–95, Feb. 2015. [Online]. Available: <https://doi.org/10.1016/j.tins.2014.11.006>
- [8] A. Schnitzler and J. Gross, “Normal and pathological oscillatory communication in the brain,” *Nature Reviews Neuroscience*, vol. 6, no. 4, pp. 285–296, Apr. 2005. [Online]. Available: <https://doi.org/10.1038/nrn1650>
- [9] C. Jutzeler, A. Curt, and J. Kramer, “Relationship between chronic pain and brain reorganization after deafferentation: A systematic review of functional MRI findings,” *NeuroImage: Clinical*, vol. 9, pp. 599–606, 2015. [Online]. Available: <https://doi.org/10.1016/j.nicl.2015.09.018>
- [10] M. Ploner and E. S. May, “Electroencephalography and magnetoencephalography in pain research—current state and future perspectives,” *Pain*, vol. 159, no. 2, pp. 206–211, Oct. 2017. [Online]. Available: <https://doi.org/10.1097/j.pain.0000000000001087>
- [11] E. S. dos Santos Pinheiro, F. C. de Queirós, P. Montoya, C. L. Santos, M. A. do Nascimento, C. H. Ito, M. Silva, D. B. N. Santos, S. Benevides, J. G. V. Miranda, K. N. Sá, and A. F. Baptista, “Electroencephalographic patterns in chronic pain: A systematic review of the literature,” *PLOS ONE*, vol. 11, no. 2, p. e0149085, Feb. 2016. [Online]. Available: <https://doi.org/10.1371/journal.pone.0149085>
- [12] J. Levitt, M. M. Edhi, R. V. Thorpe, J. W. Leung, M. Michishita, S. Koyama, S. Yoshikawa, K. A. Scarfo, A. G. Carayannopoulos, W. Gu, K. H. Srivastava, B. A. Clark, R. Esteller, D. A. Borton, S. R. Jones, and C. Y. Saab, “Pain phenotypes classified by machine learning using electroencephalography features,” *NeuroImage*, vol. 223, p. 117256, Dec. 2020. [Online]. Available: <https://doi.org/10.1016/j.neuroimage.2020.117256>
- [13] L. A. Gemein, R. T. Schirrmeyer, P. Chrabaszcz, D. Wilson, J. Boedeker, A. Schulze-Bonhage, F. Hutter, and T. Ball, “Machine-learning-based diagnostics of EEG pathology,” *NeuroImage*, vol. 220, p. 117021, Oct. 2020. [Online]. Available: <https://doi.org/10.1016/j.neuroimage.2020.117021>
- [14] Z. J. Koles, M. S. Lazar, and S. Z. Zhou, “Spatial patterns underlying population differences in the background EEG,” *Brain Topography*, vol. 2, no. 4, pp. 275–284, 1990. [Online]. Available: <https://doi.org/10.1007/bf01129656>
- [15] F. A. Alturki, M. Aljalal, A. M. Abdurraqueeb, K. Alsharabi, and A. A. Al-Shamma'a, “Common spatial pattern technique with EEG signals for diagnosis of autism and epilepsy disorders,” *IEEE Access*, vol. 9, pp. 24 334–24 349, 2021. [Online]. Available: <https://doi.org/10.1109/access.2021.3056619>
- [16] B. Blankertz, R. Tomioka, S. Lemm, M. Kawanabe, and K. Robert Muller, “Optimizing spatial filters for robust EEG single-trial analysis,” *IEEE Signal Processing Magazine*, vol. 25, no. 1, pp. 41–56, 2008. [Online]. Available: <https://doi.org/10.1109/msp.2008.4408441>
- [17] A. Delorme and S. Makeig, “EEGLAB: an open source toolbox for analysis of single-trial EEG dynamics including independent component analysis,” *Journal of Neuroscience Methods*, vol. 134, no. 1, pp. 9–21, Mar. 2004. [Online]. Available: <https://doi.org/10.1016/j.jneumeth.2003.10.009>
- [18] A. Gramfort, “MEG and EEG data analysis with MNE-python,” *Frontiers in Neuroscience*, vol. 7, 2013. [Online]. Available: <https://doi.org/10.3389/fnins.2013.00267>
- [19] F. Pedregosa, G. Varoquaux, A. Gramfort, V. Michel, B. Thirion, O. Grisel, M. Blondel, P. Prettenhofer, R. Weiss, V. Dubourg, J. Vanderplas, A. Passos, D. Cournapeau, M. Brucher, M. Perrot, and E. Duchesnay, “Scikit-learn: Machine learning in Python,” *Journal of Machine Learning Research*, vol. 12, pp. 2825–2830, 2011.
- [20] K. K. Ang, Z. Y. Chin, H. Zhang, and C. Guan, “Filter bank common spatial pattern (FBCSP) in brain-computer interface,” in *2008 IEEE International Joint Conference on Neural Networks (IEEE World Congress on Computational Intelligence)*. IEEE, Jun. 2008. [Online]. Available: <https://doi.org/10.1109/ijcnn.2008.4634130>